

INVESTIGATION OF THERMAL DECOMPOSITION AND GASES RELEASE FROM PRE-DRYING MUNICIPAL SOLID WASTE (PMSW) VIA PYROLYSIS TECHNOLOGY

Imtiaz Ali JAMRO ^a, Salim KHOSO ^{b*}, Syeed Adnan Raheel SHAH ^a, Sadaquat ALI ^c,
Fahmeed ALI ^d, Haseeb UI HASSANE ^e

^a PhD; Department of Civil Engineering, Pak Institute of Engineering and Technology, Multan Pakistan

^b PhD; Department of Civil Engineering, Quaid-e-Awam University of Engineering, Science and Technology, Campus Larkano, Sindh, Pakistan

*Corresponding author. E-mail address: enr.salimkhoso@gmail.com

^c PhD; Department of Energy and Environment Engineering, Dawood University of Engineering and Technology Karachi, Sindh, Pakistan

^d Sustainable Green Solutions Pvt. Limited, Pakistan

^e School of Civil Engineering, Central South University, China

Received: 19.08.2022; Revised: 5.11.2022; Accepted: 7.11.2022

Abstract

Present study investigates the thermal decomposition and syngas potential of pre-drying municipal solid waste (PMSW) via pyrolysis using thermo-gravimetric (TGA) analyzer coupled with the mass spectrometer (MS). The experiments were performed at the heating rates 5 and 15°C/min. Differential thermo-gravimetric (DTG) curves exposed four conversion phases at lower heating rate and two conversion phases at higher heating rate. MS analysis of the evolved gases H₂, CO, and CH₄ revealed that the devolatilization phase played a major role during the processes. Higher H₂ generation was observed at a lower heating rate due to more contact among PMSW and process temperature. Higher CO and CH₄ were also favored at lower heating rate. Total yield of gases was found higher due to higher CO generation. For the estimation of activation energy (E_a), Flynn-Wall-Ozawa (FWO) kinetic model was applied at the conversion rates (α) ranged from 5–35. In overall, the lower heating rate supported the higher WMSW conversion as well as higher gas released during the process. Hence, this study will help to evaluate the H₂ potential of the PMSW using pyrolysis thermal technology.

Keywords: Circular Economy; Municipal Solid Waste; Waste Management; Performance; Sustainability.

1. INTRODUCTION

Municipal solid waste (MSW) is considered problematic waste generated from urban life. Worldwide, the daily MSW generation is about 3.5 million tons which is increasing rapidly with the increasing urbanization, population, and economy [1–3]. On the other hand, the energy demand has been grown promptly which necessitated to search some sustainable energy

sources. Among different energy sources, the hydrogen (H₂) has been declared as one of the best alternative due to its unique characteristics such as; zero pollution (cleaner), fast-burning, and high energy density of 122 MJ/kg [4, 5]. Improper management of MSW may cause severe risks to public health and the environment. MSW contains food, plastics, paper, cloth, and rubber components, which not only discharge the large amounts of CO₂ (greenhouse gas) emissions on

open burning/dumping sites but also contaminate the waters and soil as well [6–10]. Therefore, it is one of the most critical future tasks [6–10]; hence, an efficient method is thus required.

Currently, landfilling and incineration are the most common techniques to dispose of MSW. Both techniques have led to frequent use due to the adjusting of large MSW volumes and sufficient mass reductions [1]. However, the disadvantages, for instance; complications in operation, costly lands limitations, discharging toxic leachates (liquid), and high CH₄ emissions in case of landfilling, and producing large amounts of toxic fly ash and CO₂ emissions in case of the incineration, have left negative impacts for those techniques [1]. Pyrolysis is the thermal decomposition of organic matters at a temperature of about (400–900°C) in an oxygen-absence. As no direct air or oxygen is supplied in the process, no direct burning occurs inside the reactor, also known as the opponent of the incineration. The process starts with the thermal cracking of thermally unstable compounds at a high temperature into smaller gas molecules. A gas amalgam of thermodynamically steady crude syngas (predominately H₂ molecules) is generated by increasing the temperature. On the other hand; gasification is also considered the reliable thermochemical method, however; the use of the gasifying agent makes the process costly [11, 12]. The pyrolysis of MSW is the most efficient and reliable thermochemical method. This state-of-the-art technology can significantly be lessening the huge MSW bulk and produces the valuable gas as a byproduct which can be used as a transportation fuel [13–17]. Even though, the incineration is also a thermochemical process which uses excess oxygen pyrolysis processes use no oxygen, and in return convert the waste into to an environmentally friendly synthetic gas. Whereas on the other hand; the incineration provides the heat energy which needs further long cleanup processing for its end use [18–20]. Indeed, the pyrolysis is thermal technique to breakdown the organic part of the waste in temperature ranges ~400–900°C in an oxygen-absence environment [21–23]. As no direct oxygen or air is supplied in the process, therefore no direct burning takes place inside the reactor, also known as the opponent of the incineration. The process starts with thermal cracking of unstable organic compounds at a high temperature into smaller gases molecules of H₂ and CO.

The pyrolysis process has remained a major focus in a series of studies related to MSW along with the use of various experimental facilities such as; a fluidized bed

reactor [24, 25], a fixed bed reactor [26–28], and thermo-gravimetric analyzer (TGA) [29–33]. From all those thermal facilities, TGA is the powerful tool used to measure the online investigation of thermally decomposing solid materials such as MSW, biomass, and coal [30, 34, 35]. Many studies were conducted to explore the thermal characteristics of the most common MSW components. The pyrolysis characteristics of common MSW components and their blends in TGA were investigated to see the effect of heating rate related to the final temperature [31, 57]. Their study concluded the effect of high heating rate and final temperature on each fraction is observed as a factor in reaction rate and intensity. MSW components were investigated to examine the pyrolysis mechanism of these materials [36]. From their results, it was established that the degradation behavior of cellulosic material was improved in a mixture with PVC. TGA was used to investigate the decomposition of different MSW components using pyrolysis and gasification [30]. The results showed that the final mass fractions of materials obtained from two different environments were marginally different, hence more breakdown occurred in gasification. TGA was also used to investigate various Chinese MSW fractions through pyrolysis and gasification [29]. In their study, they concluded that at lower temperature ranges less than 500°C the pyrolysis and gasification of decomposing materials behave similarly. Whereas the temperature of more than 700°C, the conversion efficiencies improve primarily due to endothermic reactions. TGA-MS was used in pyrolysis and combustion environments of typical MSW components by number of studies [37–41]. The studies estimated the occurrence of gas components such as; H₂, CH₄, H₂O, CO, CO₂. However, all the studies were limited to provide only useful degradation information of either the single components, their interrelations, or kinetic behavior of MSW components and not capable of providing information on the released part. However, there is still lack of information on the pyrolysis of PMSW, focusing on the released gases centered heating rates.

The study mainly explores H₂ potential of pre-dried municipal solid waste through pyrolysis at different heating rates. Besides, the activation energy (E_a) calculations were estimated by applying the Flynn-Wall-Ozawa (FWO) kinetic model, which provided valuable information regarding the E_a during the processes at different conversion rates. Therefore, this study will help to investigate the qualitative and quantitative analysis of pre-dried MSW for the energy potential and the performance of pyrolysis technology.

Table 1.
Proximate and ultimate analyses of PMSW

Sample	Proximate Analysis (Wt. % db)				Ultimate Analysis (Wt. % db)				
	Moisture content	Volatile matters	Fixed carbon*	Ash	C	H	O*	N	S
PMSW	11.54	72.28	5.8	10.38	59.86	6.13	32.39	0.61	1.01

Wt. %-weight percentage, db-dry basis, * by difference

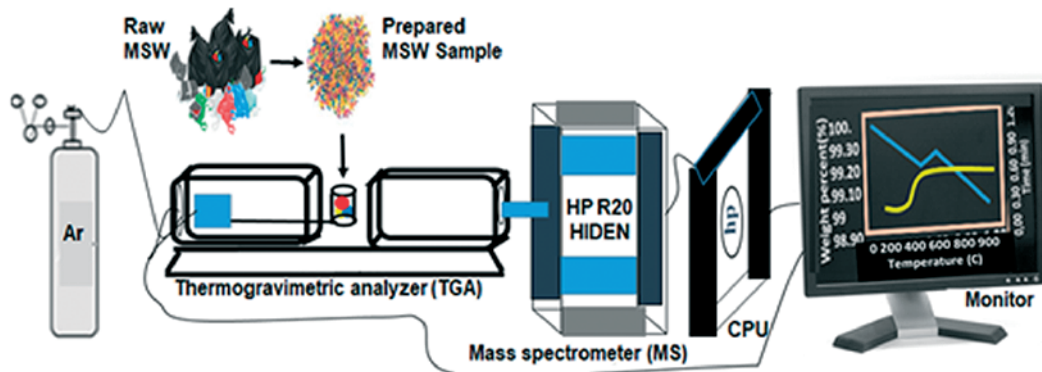


Figure 1.
TGA-MS setup for pyrolysis of the PMSW

2. MATERIALS AND METHODS

2.1. Collection and preparation of the PMSW

The pre-drying municipal solid waste (PMSW) was collected from dumping sites. The composition of PMSW consisted of food waste, polymeric plastics, paper, cloth pieces, and rubber pieces. The materials contained food (food residue, fruit peels, and vegetable trimmings), plastics (disposable bottles used for water, soft drink, juices, disposal food boxes, and soft drinks, food spoon, and forks, polythene service bags, biscuits wrappers, chips wrappers, straws, binding sticking tape), paper (cardboard boxes, marketing/advertisement brochures, product booklets, cigarette packet, stickers on cardboard, tissue paper, disposal plates), biomass (tree and plant leaves, disposal chopsticks, walnut shells, yard trimming), and rubber (tire pieces, broken chapel pieces, and tube residues). Initially, the collected materials were air-dried for 3 days and then shredded into smaller pieces. Then, a mixture of individuals was prepared with a mass ratio of 48:29:13:7:3 for food waste, polymeric plastics, paper, cloth pieces, and rubber pieces. To achieve optimal results, the pulverized materials were homogenized and sieved to average particle size to 1 mm and then kept in an oven for 12 hours at 105°C. The ready-mixed sample was then put in a desiccator until further experiments and/or their characterization.

2.2. Physical and Chemical Characteristics

The proximate analysis encompassed the contents of water volatiles and ash present in the PMSW. The elemental (chemical) composition (wt. %) was carried out by using an elemental analyzer (model 2400), by which the quantities of elemental carbon, hydrogen, sulfur, and nitrogen were examined. The oxygen and fixed carbon were computed by the difference method. The results of the proximate and ultimate analysis are shown in Table 1.

2.3. TGA-MS pyrolysis of PMSW:

A thermogravimetric analyzer (TGA) coupled with a mass spectrometer (MS) was used for pyrolysis PMSW. The TG-MS experimental setup is shown in Fig. 1.

The aim was to investigate the weight loss and the gas species evolved during the process, therefore the small weight of about 8 mg was used in all the experiments for the optimal results [26, 58]. The lower heating rates were selected to assist the release of the compounds with the lower molecular weight. To minimize the systematic errors and to establish the baseline, one blank test was conducted prior to the experiments at the heating rates 5 and 15°C/min. The metered sample was loaded in a crucible in TGA, and then each sample was kept under an isothermal con-

dition at 30°C for an hour. Afterwards, the targeted samples were pyrolyzed from room temperature to 900°C at smooth heating rates of 5 and 15°C/min. Argon (Ar) with a flow rate of 500 mL min⁻¹ was supplied. The heated capillary collected the mixture of releasing gases from TGA and conveyed it to MS to analyze and define the arrangement of the released components. In this manner, evolved gas species can be easily identified online. To attain effective results, each experiment was repeated to ensure reproducibility.

MS ionized the volatile species evolved during the thermal breakdown of sample interfaced with TGA. The heated capillary related to TGA supplied identical ions in the form of signals to the MS. Therefore, those received ions were identified and distinguished based on their mass-charge (m/z) ratios. The m/z ratios for hydrogen, methane, steam carbon monoxide, ethane, Argon (Ar), and carbon dioxide are detailed in Table 2. Ar (m/z = 40) was set as a degree to assure the consistency of the released gas components. All the mathematical calculations to determine the gas generation rate were done with documented signals applying the method reported through many studies [42, 43]. The unidentified signals were normalized by the equation below.

Normalized signals for key molecule fragmentations

$$"i" = \frac{IC_i * 500}{IC_{Ar} * Wt_{pre-drying}} \quad (1)$$

Where, IC_i shows the molecular m/z signals for molecular ion fragments "i" (arbitrary unit), Argon (Ar) flow rate of 500 ml min⁻¹ during the isothermal period IC_{Ar} is the m/z signals for Ar, and Wt_{pre-drying} MSW is the weight of the PMSW sample (mg).

Table 2.
Representative gas species evolved and key ion fragments according to their m/z ratio

Representative species	Ion fragments	m/z ratio
Hydrogen	H ₂ ⁺	2
Methane	CH ₃ ⁺	15
Water	H ₂ O ⁺	18
Carbon monoxide	CO ⁺	28
Ethane	C ₂ H ₂ ⁺	28
Argon	Ar ⁺	40
Carbon dioxide	CO ₂ ⁺	44

2.4. Kinetic Analysis

The kinetics gives valuable knowledge for the design and optimization of thermal apparatuses. Meanwhile, it calculates the weight loss performance, chemistry of the solid products, distribution of the products, and heat transfer information of the equipment [44, 45]. For kinetic assessment, two methods can be applied as isothermal and non-isothermal. Comparatively, the non-isothermal is considered the easier method due to preventing the variations of physical and chemical characteristics of the sample and giving useful information through a minimum number of experiments [46, 47]. Hence the conversion degree (α) can be calculated from experimental data by using the equation as follows:

$$\alpha = \frac{w_0 - wt}{w_0 - wf} \quad (2)$$

Where w₀ is sample mass at the starting point, wt. is the mass of PMSW at a time and temperature T, and wf is mass leftover after the reaction.

In the case of non-isothermal, the mass of any feedstock is metered as a function of temperature deviates with the time T=T(t). Therefore, heating rate (β) may be stated as;

$$\beta = dT/dt \quad (3)$$

At a linear temperature, the β is the independent function such as fractional conversion function f(α) and temperature function k(T), so the kinetic can be described as;

$$\frac{d\alpha}{dt} = \beta \frac{d\alpha}{dT} = k(T)f(\alpha) \quad (4)$$

The rate constant (k) on the temperature can be calculated via the Arrhenius expression.

$$k(T) = A \exp\left(-\frac{E_a}{RT}\right) \quad (5)$$

Where A is the pre-exponential factor (s⁻¹) E_a is the activation energy Jmol⁻¹, and R the gas constant 8.314 kJmol⁻¹.

By merging Eqns. (4) and (5), the reaction rate may be given as follows:

$$\frac{d\alpha}{dT} = \left(\frac{A}{\beta}\right) \exp\left(-\frac{E_a}{RT}\right) f(\alpha) \quad (6)$$

Integrating to Eq. (6) can be solved as.

$$G(\alpha) = \int_0^\alpha \frac{d\alpha}{f(\alpha)} = \int_0^T \left(\frac{A}{\beta}\right) \exp\left(-\frac{E_a}{RT}\right) dT = \left(\frac{AE_a}{\beta R}\right) P(x) \quad (7)$$

G(α) and P(x) are the integrated form of fractional conversions and temperature integrals. So, here P(x)

may be written as;

Here $x = \frac{Ea}{RT}$ and $P(x)$ denotes the temperature integral as:

$$P(x) = \int_x^\infty -\left(\frac{\exp(-x)}{x^2}\right) dx \quad (8)$$

Based on the integral and differential form of Eqn. (6), the kinetic parameter activation energy can easily be calculated through Flynn-Wall-Ozawa (FWO) method. FWO is an approximate integration technique ensuing from the Doyle equation. It has been effectively applied in the inquiry of non-isothermal calculations. Using FWO, the E_a can be enthusiastically determined to agree to a specified α and the lack of any information regarding the reaction [48–50]. As a result, this technique may be employed to investigate the value of E_a with the assumption of the reaction mechanism.

Through the FWO technique, Eqs. (6–7) can be transfigured into:

$$\ln\beta = \ln\left[\frac{AEa}{RG(\alpha)}\right] - 2 \ln\left(\frac{Ea}{RT}\right) - \left(\frac{Ea}{RT}\right) \quad (9)$$

Where $G(\alpha)$ is a constant at a specified α ; however; $2 \ln\left(\frac{Ea}{RT}\right)$ changes with some degree of range. Though $P(x)$ does not have the precise solution, therefore, it is approached by Doyle’s expression through the FWO model as:

$$P(x) = 0.00484 * \exp(-1.0516x) \quad (10)$$

Consequently, Eq. (9) is transformed in the FWO method as below.

$$\ln\beta = \ln\left[\frac{AEa}{RG(\alpha)}\right] - 5.331 - 1.052 \frac{Ea}{RT} \quad (11)$$

Noticeably, making $\log\beta$ versus $\frac{1}{T}$ should provide the linear plots, and the E_a may be directly computed commencing to the gradient at conversion rate points $\alpha = 5$ to 35.

3. RESULTS AND DISCUSSION

3.1. Thermal Decomposition Analysis

The quantitative information of the decomposed solid sample is commonly presented by thermogravimetric (TG) and differential thermo-gravimetric (DTG) thermographs. TG shows the total conversion (weight loss) in percentage (%) as an inclined curve, whereas; the DTG shows the rate of conversion ($d\alpha/dt \text{ min}^{-1}$) as peaks at specific temperature ranges. TG and DTG profiles for the non-isothermal pyrolysis of the biomass at heating rates; 5 and 15°C/min

are presented in Fig. 2. Pyrolysis of disintegrating solid mass is a diverse process that usually involves three specific temperature sub-processes: evaporation, primary decomposition, and secondary decomposition [47, 59]. In the 1st (evaporation) stage, the free moisture and some unstable hydrocarbons are released in the temperature range 100–200°C, resulting in minor weight loss mainly depending on nature and the conditions of the process. In the 2nd stage, the devolatilization (primary decomposition), the release of unstable polymers-plastics and biopolymers-biomass has occurred in the temperature range ~172–532°C. This stage is accounted for the major loss in weight therefore sometimes also known as the active stage of the pyrolysis. In the 3rd (secondary decomposition) stage, which begins from the end of the active stage, a secondary breakdown of the sample results in char formation and the char formation reactions sustained up to upper temperatures of the process. In the secondary phase, minor weight losses are achieved over the primary phase hence this stage is known as a passive stage. The 2nd and 3rd phases were found to depend on each other, primarily on the general chemical composition of the reacting solid, specifically the structural bonding. The substantial decomposition of ~43% and 39% occurred in the devolatilization phase in the temperature ranges of 200–700°C and 200–510°C at 5 and 15°C/min respectively obviously due to the presence of higher volatiles in the mixture. Below 200°C, the TG curves (Fig. 2a) under both the heating rates showed a similar weight loss ~ 3% i.e. witnessed the presence of a smaller quantity of water in the samples. Under low heating rate, the sample reached its maximum decomposition of 47% at temperature ~716°C whereas at a higher heating rate, the decomposition of 43% at temperature 737°C. Henceforth, the lower heating rate exhibited higher decomposition ~4% than the higher heating rate. Very similar observations of weight loss at the primary and final phases were also reported by [51, 60] during the co-pyrolysis of a binary mixture of two plastics; hence our sample was also the mixture of several types of plastics. TG pyrolysis profiles of the PMSW samples for both the heating rate are illustrated in Fig. 2a.

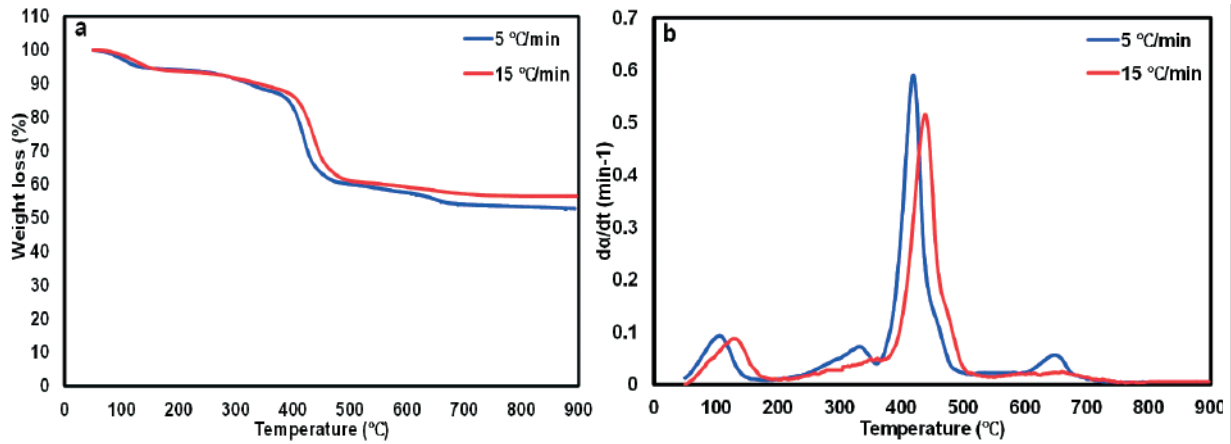


Figure 2. Thermogravimetric (TG) and Differential thermo-gravimetric (DTG) (b) profiles of pyrolysis of PMSW

Table 3. Temperature characteristics of the conversion phases obtained from pyrolysis of PMSW

Regime	Heating rate (°C/min)	Stage 1			Stage 2			Stage 3			Stage 4		
		T _i (°C)	T _{max} (°C)	T _f (°C)	T _i (°C)	T _{max} (°C)	T _f (°C)	T _i (°C)	T _{max} (°C)	T _f (°C)	T _i (°C)	T _{max} (°C)	T _f (°C)
Pyrolysis	5	50	113	180	230	334	360	360	419	500	605	652	690
	15	50	133	182	230	438	515	-	-	-	-	-	-

Note: T_i is the initial temperature of each phase; T_{max} is the maximum (at peak) temperature of each phase; T_f is the final temperature of each phase

Differential thermogravimetric (DTG) thermographs of the PMSW samples at both the heating rates are shown in Fig. 2b. For low heating rate, the four conversion phases were observed in the temperature ranges from 50–180°C, 230–360°C, 360–500°C, and 605–690°C. However, only two conversion phases were observed at the lower heating rate in the temperature ranges from 50–182°C and 230–515°C. In the first conversion phase, both samples followed almost the same .i.e., small decomposition profile for water removal ~3% in the temperature ranges from 50–180°C and 50–182°C for each heating rate. The devolatilization, commonly represented by second and third conversion phases, behaved differently; however, it showed a major weight loss at both heating rates. For lower heating rates, the second and third conversions conjointly represented the devolatilization (primary decomposition) between 230–530°C, henceforth cause to a major loss in weight ~43%. On the other hand, the pyrolysis at a higher heating rate, the thermal conversion stratagem of the PMSW sample was completely different; henceforth could reach only up to the 2nd conversion phase with the total weight loss ~39% and left 56% as unreacted part. The reason behind the two conversion phases for higher heating rate instead of four in case of

the lower heating rate attributed to the sample minimum residence time even under the same process condition. In addition, at a higher heating rate, several blurring (dull) peaks were demonstrated in the temperature ranges from 220–380°C, and 550–690°C evidenced that the sample endeavoured to decay under fast heating just penetrated it partially, hence degraded slightly less. Whereas, under the lower heating rate condition, the decomposition process continued and entered the fourth conversion phase. The fourth (secondary decomposition) conversion phase is known for some char formation and its decomposition. In this phase, the decomposition of ~1.5–2% in the temperature range from 605–690°C occurred, hence strongly attributed to the self-gasification of char which was not achieved at higher heating rate. The final residue from the fourth conversion phase was approximately 53% as char. The pyrolysis results of PMSW at two different heating rates reported that the maximum residence time permits more heat entry into the innermost core of the solid particles in the case of moderate and/or slow heating. On the contrary, there was insufficient heat entry; hence, less decomposition occurred at fast heating. Overall, the lower heating rate DTG curves exposed the PMSW decomposition in four conversion phases.

The devolatilization region ascertained itself the most influential weight loss phase. The details of the conversion phases at the applied heating rates are given in Table 3.

3.2. Released Gases Analysis

The gas generation trends present the qualitative information of any decomposed solid sample during thermal degradation, which can easily be determined by a mass spectrometer (MS). MS identifies the ion intensity of each gas specie based on their mass to charge (m/z) ratio. A semi-quantitative approach that effectively works based on signals corresponding to each ion fragment was used to assess the gas arrangement during both processes [30, 31]. The release of detected common fragments included; H₂, CH₄, C₂H₂, CO, and CO₂. The aim was to investigate only combustible gases; hence CO₂ was excluded. In addition, the concentration of C₂H₂ was too little to be appropriately displayed; therefore, it was also excluded. Fig. 3 depicts the generation rates of H₂, CO, and

CH₄ and their yields obtained from pyrolysis of PMSW at the heating rates of 5 and 15°C/min. As the sample contained a considerable amount of plastics (29% share) and lignocellulosic components, the pyrolytic decomposition followed the decay profile via a radical mechanism for plastics, whereas a chain of exothermic endothermic nature of reactions for the lignocellulosic fraction.

The H₂ generation trends of the pyrolysis of the PMSW are illustrated in Fig. 3a. For both heating rates, the generation of H₂ was elevated from 0.5 to 4 ml min⁻¹ g⁻¹ in the temperature ranges from 400–430°C but suddenly decreased to 2 ml min⁻¹ g⁻¹ at 500°C. Afterwards, a rapid increment from 2 ml min⁻¹ g⁻¹ to 12 ml min⁻¹ g⁻¹ and 2 ml min⁻¹ g⁻¹ to 9 ml min⁻¹ g⁻¹ was observed in the temperature ranges 500–760°C and 500–710°C for lower heating rate and higher heating rate, respectively.

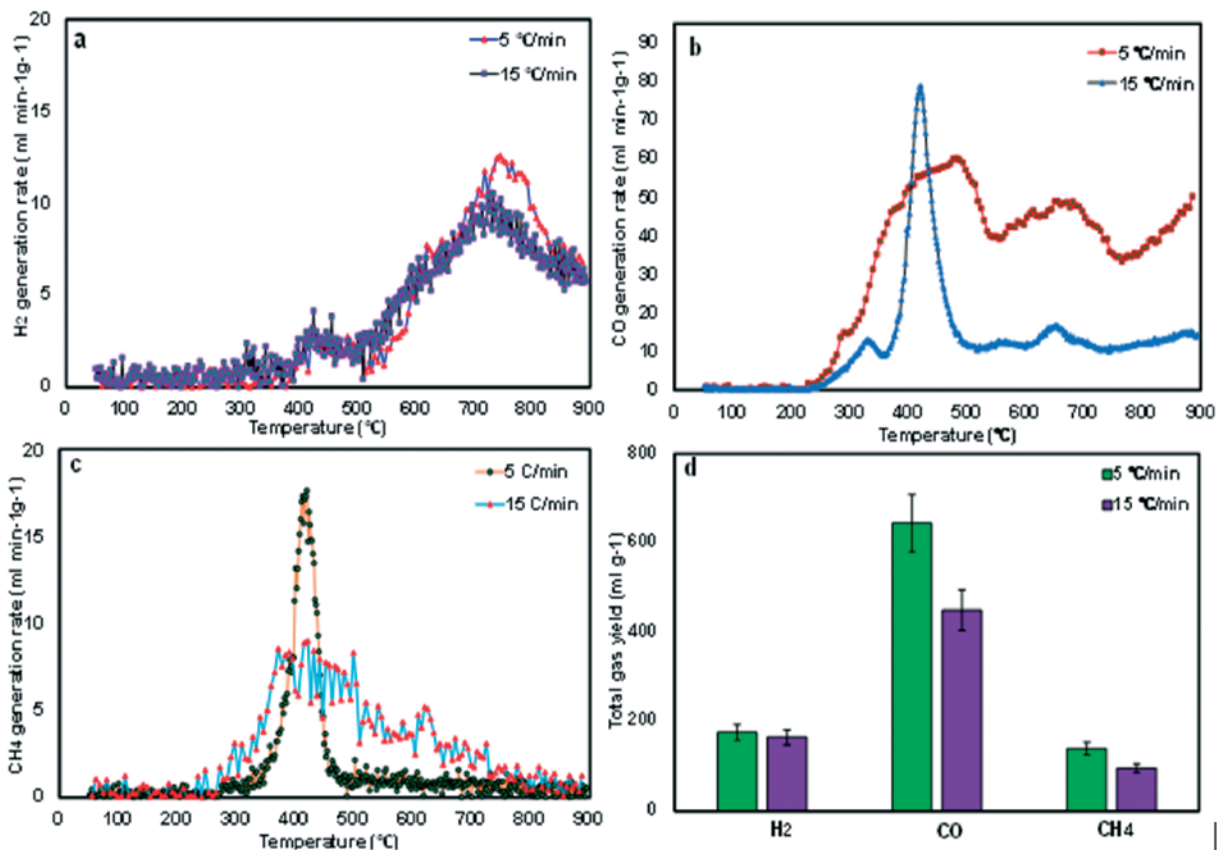


Figure 3. The generation rates of (a) H₂, (b) CO, and (c) CH₄, and (d) their total yields obtained from pyrolysis of PMSW at 5 and 15°C/min.

It is strongly believed that the H₂ production is mainly occurred due to the primary cracking of hydrocarbons and their subsequent decomposition reactions [34, 47]. According to [52, 53], the upper-level temperature provides favorable circumstances to the thermal disintegration of carbon-carbon bonds hence; high probability of water gas shift and reforming of methane reactions has occurred, resulting in the boosted H₂ production. Apart from that, the secondary cracking of char/ash catalytic assistance by the paper and biomass fractions in the mix might be contributed to augmenting the H₂ generation. This fluctuating phenomenon for the H₂ generation is likely to be processed via water-gas shift, water gas, and steam methane reforming reactions. From low to higher heating rate, the H₂ generation rate was decreased after 760°C and 710°C which continued till the end of the process. The results acquired for H₂ are in good agreement with the study conducted on individual components such as; paper, plastics, yard trimmings in the pyrolysis atmosphere [29]. In conclusion, the H₂ generation from the pyrolysis of the PMSW was slightly favoured by the lower heating rate over the higher heating rate.

The CO presented different generation trends at both heating rates, as indicated in Fig. 3b. At a lower heating rate, the CO generation increased from 10 to 62 ml min⁻¹ g⁻¹ in the temperature range from 230–500°C and reached its maximum level. There was a clear shoulder displayed at 300°C in the temperature range from 290–310°C, which then ascended and merged with the ongoing trend line. After reaching its maximum peak level, a combination of decreasing and increasing trends persisted up to 800°C. Notably, after touching 800°C to the final process temperature i.e. 900°C, the generation trend remained in a constantly increasing position. On the other hand, at the higher heating rate the CO generation trend increased from 5 to 78 ml min⁻¹ g⁻¹ in the temperature range from 250–420°C and reached at its maximum level. A little peak was observed at 330°C in the ranges 290–310°C. At that moment, the trend line suddenly dropped from 78 to 12 ml min⁻¹ g⁻¹ and that declination continued till the end of the process. The similar resembling CO fluctuating trend also reported for the pyrolysis of polystyrene plastic component which first increased with the elevating temperature and suddenly decreased at higher temperatures [37]. A similar higher CO generation was also reported by the other researchers for the lingo-cellulosic (biomass) and/or cellulosic originated (paper) materials

in the PMSW mixture [34, 37]. Hence, the thermal disintegration of ether bonds, carboxyl, and carbonyl groups exist in hemicellulose and cellulose, resulting in higher CO generation hence the results well agreed with the previous studies [54, 55]. On the other hand, the phenomenon of the lower CO generation at the lower heating rate could have also changed due to the primary reaction, essentially the gradual improvement in H₂ and CO₂ associated with the marginal catalytic characteristics of ashes [56]. The evolution of CH₄ generation followed relatively parallel generation trends i.e. higher generation rate at the lower heating rate and lower at the high heating rate as illustrated in Fig. 3c. At a lower heating rate, the CH₄ generation increased from 4 ml min⁻¹ g⁻¹ to 18 ml min⁻¹ g⁻¹ in temperatures 300–400°C. But, a quick leaping was observed in the temperature range 400–470°C, which reached its lowest generation level of 2 ml min⁻¹ g⁻¹ to the end of the process. For the high heating rate, the trend was the same as the lower heating rate, but it could only reach half of the maximum level of lower heating rate, i.e., around 9 ml min⁻¹ g⁻¹ in 290–410 °C ranges. In addition, several peaks were seen which showed the inconsistency of pyrolytic decomposition under the higher heating rate. Overall, the H₂ generation was merely slow for a lower heating rate, which decreased from 750°C to the end. On the other hand, the higher heating rate pyrolysis produced the maximum CO generation after 300°C, increasing continuously. The low heating rate took a wide span of CH₄ increment between 320–490°C. Regarding the higher heating rate, the CH₄ generation increased between 300–500°C, and the decreasing trend continued till the end of the process. The total yield of the released gases is shown in Fig. 3d. Overall, the lower heating rate favoured the high total yield for all the gases i.e. H₂, CO, and CH₄. However, a minor difference in the total yield was observed for the H₂. The CO owned the highest total yield in the temperature ranges 230–500°C and 800°C to end of the processes temperature i.e. 900°C.

3.3. Kinetics Analysis

To check the energy required in the weight loss of PMSW during pyrolysis, the estimation of kinetic parameters is essential, calculated by the Arrhenius equation. The TGA results were evaluated by the model-free fitting method to calculate the kinetic parameters. Afterwards, the temperatures parallel to fixed values of conversion degree (α) from experiments at the applied heating rates were obtained. In

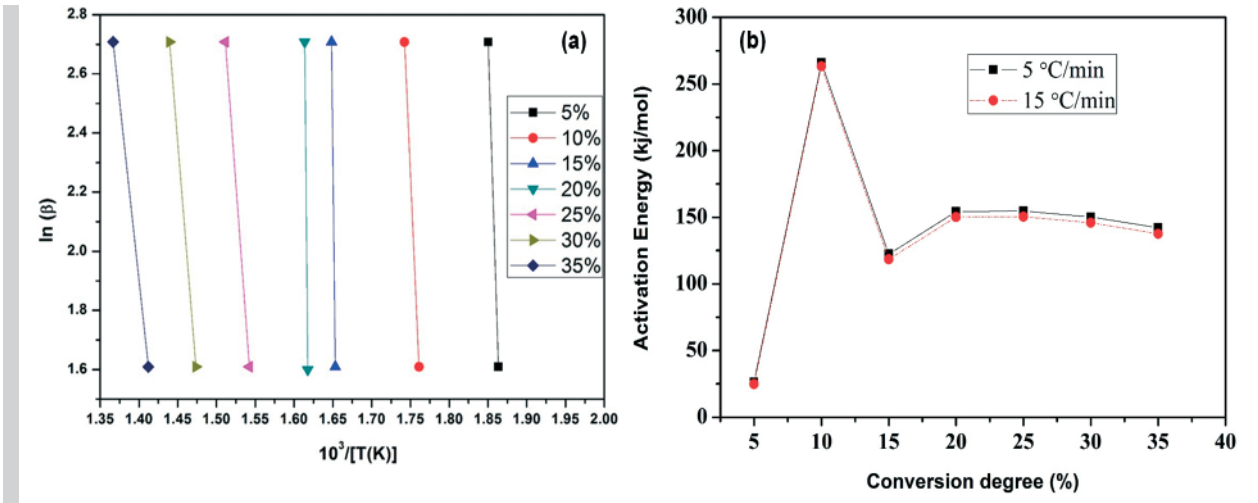


Figure 4. (a) Fitting curves and (b) plots of activation energy obtained from the pyrolysis of PMSW at different conversion degrees at heating rates of 5 and 15°C/min.

this study, the activation energy (Ea) was estimated by the non-isothermal iso-conversion technique by Flynn-Wall-Ozawa (FWO) and employing Doyle’s approximation of p(x) as follows:

$$\log \beta = \log \left[\frac{AEa}{RG(\alpha)} \right] - 2.315 - 0.4567 \frac{Ea}{RT} \quad (12)$$

Fig. 4a represents the fitting curve plots of ln(β) versus 10³/T corresponding to the different conversion degrees (α) at both heating rates. To calculate the Ea at a certain α that how the reaction rate varies with temperature at a particular α has to be identified; hence it can be established by changing the heating rate (β) [34, 47]. Therefore at the conversion α, the Ea can be calculated after simplifying and by taking the derivative of equation 5 concerning to $\left(-\frac{1}{RT}\right)$.

$$Ea(\alpha) = \frac{\partial \ln\left(\frac{d\alpha}{dt}\right)_{\alpha,j}}{\partial (-RT_{\alpha,j})^{-1}} \quad (13)$$

Where the subscript j means the heating program selected, hence the obtained Ea are recorded in Table 4. The obtained Ea values and model validation are schemed in Fig. 4a and Fig. 3b, respectively.

Table 4 depicts the estimated Ea values at 5 and 15°C/min heating rates. The correlation coefficient (R²) ranged from 0.9701 to 0.9983 hence; validating the generated data well. Fig. 5b depicts the lower heating rate owned higher values of Ea over higher heating rate except from the conversion rate (α) of 10 for the pyrolysis. The higher Ea values of 266 and 263 kJmol⁻¹ at both heating rates at α of 10 were found at ~295°C can be ascribed may be due to the

Table 4: Kinetic parameters at different conversion rates at heating rates of 5 and 15°C/min

Environment	Heating rate (°C/min)	Conversion degree (α)	Activation energy (kJmol⁻¹)	R²
Pyrolysis	5	5	26.2165	0.9972
		10	266.1419	0.9722
		15	122.3063	0.9967
		20	154.2912	0.9839
		25	154.6809	0.9849
		30	150.212	0.9941
		35	142.1621	0.9932
	15	5	24.89866	0.9983
		10	263.3126	0.9701
		15	118.488	0.9949
		20	150.2019	0.9811
		25	150.4602	0.9935
		30	145.8795	0.9922
		35	137.6665	0.9917

presence of plastic content in the mix, which usually starts to decompose from 290–350°C in the absence of gasifying agent required more energy. At a lower heating rate, the values of Ea lied between 26 kJmol⁻¹ to 142 kJmol⁻¹.

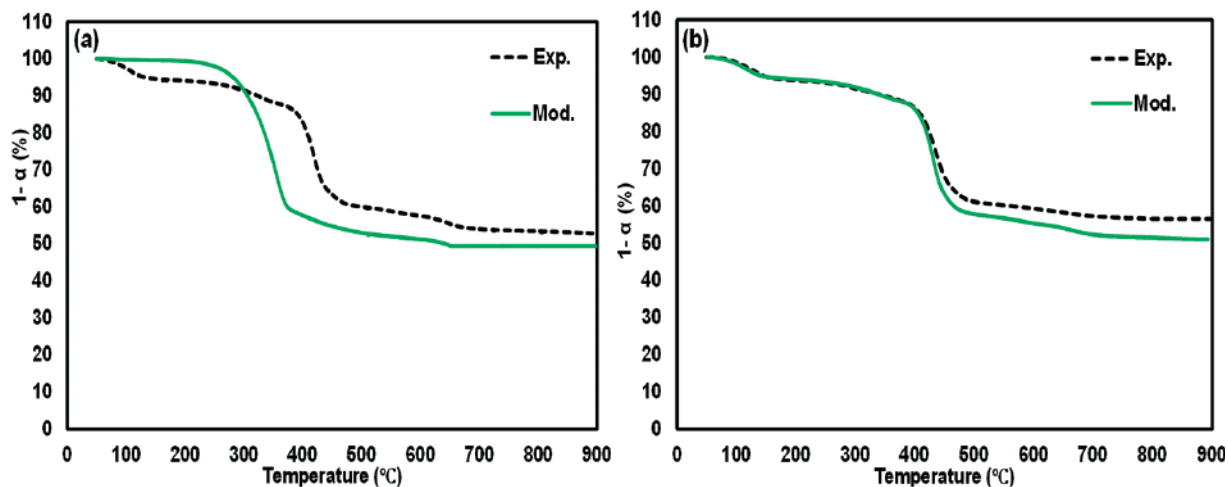


Figure 5. Experimental (dotted) and model (solid) lines through the FWO method were (a) and (b) show the pyrolysis at 5 and 15°C/min, respectively

Comparatively, the E_a values estimated in our study for the PMSW are less than the individual MSW components i.e. hemicellulose, cellulose, lignin, polyethylene, and polystyrene ranged between 171–221 kJmol⁻¹ [30]. Hence this work has demonstrated that the pyrolysis of PMSW at 5 and 15°C/min pay considerable value in terms of E_a related to the thermal behaviour of the PMSW. From the validation of model curves as depicted in Fig. 5, it may be seen that the FWO model provides an agreeable reproducibility to the experimental results throughout all the conversion degrees. Nevertheless, higher deviations among the calculated and experimental information may be seen at 5°C/min between the conversion degree of 5 and 25. The experimental and calculated curves trend was smooth and overlapped, hence correspondingly following the same pathway along the trajectory. The experiment curves at 5°C/min (Fig. 4a) had certain discrepancies with calculated curves along the same trajectory in the ranges about 300–500°C, thus appearing as slow and continued fluctuating curves presenting slower and minimum decomposition. While the calculated curves at 15°C/min (Fig. 4b) exhibited smooth experimental and calculated curves with persistent flat parallel curves. In summary, the pyrolysis of PMSW was observed to be slower than the deviation among the PMSW with identical conditions was strongly linked to the heating rates.

4. CONCLUSIONS AND FUTURE DIRECTIONS

Pyrolysis of pre-drying municipal solid waste (PMSW) in terms of degradation, evolved gases, and kinetics under two heating rates of 5 and 15°C/min, and final temperature of 900°C was carried out by using a thermogravimetric analyzer (TGA) coupled with a mass spectrometer (MS). The TG (thermal decomposition) results revealed that the lower heating rate was more efficient in more conversion of the feedstock. Total weight loss and rate of weight loss provided logical information under identical conditions. Hence, the final weight loss of about 47% was obtained at the lower heating rate and 43% weight loss at a higher heating rate. On the other hand, the DTG curves revealed how exactly the material degraded in different conversion phases was associated with the specific range of temperatures. For higher H₂ generation, the lower heating rate produced higher H₂ and reached its maximum generation level after 800°C. Such increment in H₂ generation at higher temperatures was considered mainly due to water gas shift and steam-methane reforming reactions supported at higher temperatures. In addition, the lower heating rate produced also produced higher gas yields over the higher heating rate. In the case of H₂ as the desired product, which was found as temperature contingent species, i.e., increased with the increasing temperatures. The kinetic results revealed that the activation energy (E_a) values at lower heating rate lied between 26–142 kJmol⁻¹, whereas for higher heating rate, the E_a values ranged between

24–137 kJmol⁻¹, respectively. Henceforth, it can be established that pyrolysis of PMSW is not an economical process for tending to produce cleaner and expensive H₂ production but also a perfect deal to manage the MSW. As MSW is a sustainable, renewable, and permanent source; hence, the current study may help in its safe management and fulfil future energy requirements. In addition, the releasing H₂ tends may also help to perform the pyrolysis of PMSW at real reactors (fixed bed, tubular batch) for the future work and its use as an appropriate fuel for Fischer Tropsch process for the manufacturing of transportation oils.

REFERENCES

- [1] Zhou, H., et al. (2014). An overview of characteristics of municipal solid waste fuel in China: physical, chemical composition and heating value. *Renewable and sustainable energy reviews*, 36, 107–122.
- [2] Pan, A., L. Yu, and Q. Yang (2019). Characteristics and forecasting of municipal solid waste generation in China. *Sustainability*, 11(5), 1433.
- [3] Mian, M.M., et al. (2017). Municipal solid waste management in China: a comparative analysis. *Journal of material cycles and waste management*, 19(3), 1127–1135.
- [4] Ji, G., et al. (2017). Enhanced hydrogen production from sawdust decomposition using hybrid-functional Ni-CaO-Ca₂SiO₄ materials. *Environmental Science & Technology*, 51(19), 11484–11492.
- [5] Raheem, A., et al. (2018). Catalytic gasification of algal biomass for hydrogen-rich gas production: parametric optimization via central composite design. *Energy Conversion and Management*, 158, 235–245.
- [6] Rada, E.C., et al. (2018). Dioxin contamination after a hypothetical accidental fire in baled municipal solid waste storage. *environment*, 17, 21.
- [7] Khandelwal, H., et al. (2019). Application of life cycle assessment in municipal solid waste management: A worldwide critical review. *Journal of Cleaner Production*, 209, 630–654.
- [8] Cocarta, D., et al. (2009). A contribution for a correct vision of health impact from municipal solid waste treatments. *Environmental technology*, 30(9), 963–968.
- [9] Giusti, L. (2009). A review of waste management practices and their impact on human health. *Waste management*, 29(8), 2227–2239.
- [10] Kanchanabhan, T., et al. (2011). Application of geographical information system (GIS) in optimisation of waste collection for Alandur Municipality in South Chennai, India. *International Journal of Environment and Waste Management*, 7(3-4), 395–410.
- [11] Young, G.C. (2010). Municipal solid waste to energy conversion processes: economic, technical, and renewable comparisons. John Wiley & Sons.
- [12] McGowan, T. (2010). Municipal Solid Waste to Energy Conversion Processes: Economic, Technical and Renewable Comparisons. *Chemical Engineering*, 117(12), 8–10.
- [13] Chen, L., et al. (2018). Co-pyrolysis kinetics and behaviors of kitchen waste and chlorella vulgaris using thermogravimetric analyzer and fixed bed reactor. *Energy Conversion and Management*, 165, 45–52.
- [14] Van Nguyen, Q., et al. (2021). Co-pyrolysis of coffee-grounds and waste polystyrene foam: Synergistic effect and product characteristics analysis. 292, 120375.
- [15] Lopez, G., et al. (2017). Thermochemical routes for the valorization of waste polyolefinic plastics to produce fuels and chemicals. A review. *Renewable and Sustainable Energy Reviews*, 73, 346–368.
- [16] Lopez, G., et al. (2018). Recent advances in the gasification of waste plastics. A critical overview. *Renewable and Sustainable Energy Reviews*, 82, 576–596.
- [17] Plastics. Plastics – the Facts 2016: An Analysis of European Plastics Production, demand and waste data. Brussels – Belgium. 2021 [cited 2020 August 17]; Available from: <https://plasticseurope.org/wp-content/uploads/2021/10/2016-Plastic-the-facts.pdf>.
- [18] Kai, X., et al. (2019). TG-FTIR-MS study of synergistic effects during co-pyrolysis of corn stalk and high-density polyethylene (HDPE). *Energy Conversion and Management*, 181, 202–213.
- [19] Sharuddin, S.D.A., et al. (2016). A review on pyrolysis of plastic wastes. *Energy conversion and management*, 115, 308–326.
- [20] Kunwar, B., et al. (2016). Plastics to fuel: a review. *Renewable and Sustainable Energy Reviews*, 54, 421–428.
- [21] Abnisa, F., et al. (2013). Co-pyrolysis of palm shell and polystyrene waste mixtures to synthesis liquid fuel. *Fuel*, 108, 311–318.
- [22] Brebu, M., et al. (2010). Co-pyrolysis of pine cone with synthetic polymers. *Fuel*, 89(8), 1911–1918.
- [23] Özsın, G. and A.E. Pütün (2017). Insights into pyrolysis and co-pyrolysis of biomass and polystyrene: Thermochemical behaviors, kinetics and evolved gas analysis. *Energy Conversion and Management*, 149, 675–685.
- [24] Liu, Y., J. Qian, and J. Wang (2000). Pyrolysis of polystyrene waste in a fluidized-bed reactor to obtain styrene monomer and gasoline fraction. *Fuel Processing Technology*, 63(1), 45–55.
- [25] Jin, Y. (2002). Study on MSW combustion characteristics and a new CFB incineration technology. Hangzhou: Zhejiang University.

- [26] Luo, S., et al. (2010). Effect of particle size on pyrolysis of single-component municipal solid waste in fixed bed reactor. *International journal of hydrogen energy*, 35(1), 93–97.
- [27] Zhang, Q., et al. (2012). Gasification of municipal solid waste in the Plasma Gasification Melting process. *Applied Energy*, 90(1), 106–112.
- [28] Lopez-Velazquez, M., et al. (2013). Pyrolysis of orange waste: a thermo-kinetic study. *Journal of Analytical and Applied Pyrolysis*, 99, 170–177.
- [29] Chen, S., et al. (2015). TGA pyrolysis and gasification of combustible municipal solid waste. *Journal of the energy institute*, 88(3), 332–343.
- [30] Meng, A., et al. (2015). Pyrolysis and gasification of typical components in wastes with macro-TGA. *Waste management*, 46, 247–256.
- [31] Zheng, J., et al. (2009). Pyrolysis characteristics of organic components of municipal solid waste at high heating rates. *Waste Management*, 29(3), 1089–1094.
- [32] Dawei, A., et al. (2006). Low temperature pyrolysis of municipal solid waste: influence of pyrolysis temperature on the characteristics of solid fuel. *International journal of energy research*, 30(5), 349–357.
- [33] Singh, S., C. Wu, and P.T. Williams (2012). Pyrolysis of waste materials using TGA-MS and TGA-FTIR as complementary characterisation techniques. *Journal of Analytical and Applied Pyrolysis*, 94, 99–107.
- [34] Zhao, M., et al. (2019). Iso-conversional kinetics of low-lipid micro-algae gasification by air. *Journal of Cleaner Production*, 207, 618–629.
- [35] De Caprariis, B., et al. (2012). Double-Gaussian distributed activation energy model for coal devolatilization. *Energy & Fuels*, 26(10), 6153–6159.
- [36] Sørum, L., M. Grønli, and J. Hustad (2001). Pyrolysis characteristics and kinetics of municipal solid wastes. *Fuel*, 80(9), 1217–1227.
- [37] Gunasee, S.D., et al. (2016). Pyrolysis and combustion of municipal solid wastes: Evaluation of synergistic effects using TGA-MS. *Journal of Analytical and Applied Pyrolysis*, 121, 50–61.
- [38] CE. Research helps Europe advance towards circular economy. 2021 [cited 2021 August 12]; Available from: <https://ec.europa.eu/jrc/en/news/research-helps-europe-advance-towards-circular-economy>.
- [39] Yong, Z.J., et al. (2019). Sustainable waste-to-energy development in Malaysia: Appraisal of environmental, financial, and public issues related with energy recovery from municipal solid waste. *Processes*, 7(10), 676.
- [40] UN. United Nations Economic and Social Commissions (UNESCAP) (2016). Visualization of Interlinkages for SDG 7; UNESCAP: New York, NY, USA. (accessed on 20 December 2021). Available. 2021; Available from: <https://www.unescap.org/sites/default/files/Visualisation%20of%20interlinkages%20for%20SDG%207.pdf>.
- [41] UN. GOAL 7: Affordable and Clean Energy; UN Environment: Nairobi, Kenya, 2019. 2021 [cited 2021 December 25]; Available from: <https://www.unep.org/explore-topics/sustainable-development-goals/why-do-sustainable-development-goals-matter/goal-7>.
- [42] Zhao, M., N.H. Florin, and A.T. Harris (2009). The influence of supported Ni catalysts on the product gas distribution and H₂ yield during cellulose pyrolysis. *Applied Catalysis B: Environmental*, 92(1-2), 185–193.
- [43] Zhao, M., N.H. Florin, and A.T. Harris (2010). Mesoporous supported cobalt catalysts for enhanced hydrogen production during cellulose decomposition. *Applied Catalysis B: Environmental*, 97(1-2), 142–150.
- [44] Abd Aziz, M.F.S. and Z.A. Zakaria (2018). Oil Palm Biomass and Its Kinetic Transformation Properties, in *Biosynthetic Technology and Environmental Challenges*. Springer, 73–87.
- [45] Mishra, R.K. and K. Mohanty (2018). Pyrolysis kinetics and thermal behavior of waste sawdust biomass using thermogravimetric analysis. *Bioresource technology*, 251, 63–74.
- [46] Zhang, Q., et al. (2017). Experimental study on co-pyrolysis and gasification of biomass with deoiled asphalt. *Energy*, 134, 301–310.
- [47] Özsın, G. and A.E. Pütün (2019). TGA/MS/FT-IR study for kinetic evaluation and evolved gas analysis of a biomass/PVC co-pyrolysis process. *Energy conversion and management*, 182, 143–153.
- [48] Huang, Z., Q.-q. Ye, and L.-j. Teng (2015). A comparison study on thermal decomposition behavior of poly (l-lactide) with different kinetic models. *Journal of Thermal Analysis and Calorimetry*, 119(3).
- [49] Jain, A.A., A. Mehra, and V.V. Ranade (2016). Processing of TGA data: Analysis of isoconversional and model fitting methods. *Fuel*, 165, 490–498.
- [50] Ali, M., et al. (2018). The effect of hydrolysis on combustion characteristics of sewage sludge and leaching behavior of heavy metals. *Environmental technology*, 39(20), 2632–2640.
- [51] Zhou, H., et al. (2015). Thermogravimetric characteristics of typical municipal solid waste fractions during co-pyrolysis. *Waste management*, 38, 194–200.
- [52] Figueira, C.E., P.F. Moreira Jr, and R. (2015). Giudici, Thermogravimetric analysis of the gasification of microalgae *Chlorella vulgaris*. *Bioresource technology*, 198, 717–724.
- [53] López-González, D., et al. (2014). Comparison of the steam gasification performance of three species of microalgae by thermogravimetric–mass spectrometric analysis. *Fuel*, 134, 1–10.
- [54] Ridout, A.J., M. Carrier, and J. Görgens (2015). Fast pyrolysis of low and high ash paper waste sludge: Influence of reactor temperature and pellet size. *Journal of analytical and applied pyrolysis*, 111, 64–75.

- [55] Garcia-Maraver, A., et al. (2015). Determination and comparison of combustion kinetics parameters of agricultural biomass from olive trees. *Renewable Energy*, 83, 897–904.
- [56] Cheng, K., W.T. Winter, and A.J. Stipanovic (2012). A modulated-TGA approach to the kinetics of lignocellulosic biomass pyrolysis/combustion. *Polymer degradation and stability*, 97(9), 1606–1615.
- [57] Khoso, S., Ansari, A. A., Wagan, F. H., (2014). Investigative construction of buildings using baked clay post reinforced beam panels. *Journal of Architecture Civil Engineering Environment ACEE*, 7(4), 57–66. ISSN: 1899-0142
- [58] Khoso, S., Naqash, M. T., Sher, S., & Saeed, Z. (2018). An experimental study on fiberly reinforced concrete using polypropylene fibre with virgin and recycled road aggregate. *Journal of Architecture Civil Engineering Environment*, 11, 73–80.
- [59] Khoso, S., Raad, J., & Parvin, A. (2019). Experimental investigation on the properties of recycled concrete using hybrid fibers. *Open Journal of Composite Materials*, 9(02), 183.
- [60] A Soltani, S Khoso, MA Keerio, A Formisano, (2019) “Assessment of Physical and Mechanical Properties of Concrete Produced from Various Portland Cement Brands” *Open Journal of Composite Materials* 9(04), 327.